Respiratory Physiology & Neurobiology 232 (2016) 66–74

Contents lists available at ScienceDirect

Respiratory Physiology & Neurobiology

journal homepage: www.elsevier.com/locate/resphysiol

Characterizing human nasal airflow physiologic variables by nasal index

Aniruddha Patki (MD)[a], Dennis O. Frank-Ito (PhD)[a,b,c,*]

[a] Division of Head and Neck Surgery & Communication Sciences, Duke University Medical Center, Durham, NC, USA
[b] Computational Biology & Bioinformatics Program, Duke University, Durham, NC, USA
[c] Department of Mechanical Engineering and Materials Science, Duke University, Durham, NC, USA

ARTICLE INFO

Article history:
Received 30 March 2016
Received in revised form 13 July 2016
Accepted 14 July 2016
Available online 16 July 2016

Keywords:
Nasal index
Computational fluid dynamics
Nasal resistance
Heat flux
Wall shear stress

ABSTRACT

Although variations in nasal index (NI) have been reported to represent adaptation to climatic conditions, assessments of NI with airflow variables have not been rigorously investigated. This study uses computational fluid dynamics modeling to investigate the relationship between NI and airflow variables in 16 subjects with normal nasal anatomy. Airflow simulations were conducted under constant inspiratory pressure. Nasal resistance (NR) against NI showed weak association from nostrils to anterior inferior turbinate ($R^2 = 0.26$) and nostril to choanae ($R^2 = 0.12$). NI accounted for 38% and 41% of the respective variation in wall shear stress (WSS) and heat flux (HF) at the nasal vestibule, and 52% and 49% of variability in WSS and HF across the entire nose. HF and WSS had strong correlation with NI < 80, and weakly correlated with NI > 80; these differences in HF and WSS for NI < 80 and NI > 80 were not statistically significant. Results suggest strong relationship between NI and both WSS and HF but not NR, particularly in subjects with NI < 80.

1. Introduction

The ratio of nasal width to nasal height is known as the nasal index (NI) (Crognier, 1981; Davies, 1932; Hiernaux and Froment, 1976; Thomson and Buxton, 1923; Weiner, 1954; Wolpoff, 1968). When assessing the external soft tissue (nose), NI is the ratio of the interalar width to the nasal height from subnasale to nasion. For the facial skeleton, NI is the ratio of piriform aperture width to nasal height from nasion to naso-spinale (Yokley, 2009). NI is one of the most commonly used measures to classify nasal shape by racial group (Leong and Eccles, 2009; Thomson and Buxton, 1923). Noses with NI < 70 are classified as "leptorrhine", "mesorrhine" for 70 < NI < 85, and "platyrrhine" for NI > 85. Typical Caucasian noses are taller and narrower, and belong to the leptorrhine category; while individuals of African descent typically have broader and shorter noses, are usually in the platyrrhine category (Leong and Eccles, 2009; Ohki et al., 1991; Romo and Abraham, 2003). Asian and Latin American populations generally are intermediate and in the mesorrhine category (Daniel, 2003; Leach, 2002; Leong and Eccles, 2009; Ohki et al., 1991).

Nasal morphology has long been recognized to vary by geographic region, an adaptation to diverse climatic environments (Noback et al., 2011; Weiner, 1954; Yokley, 2009). Populations with a leptorrhine nasal type (NI < 70) were more commonly found in cold and/or dry climates, while populations with platyrrhine nasal type (NI > 85) were associated with humid and warm climates (Crognier, 1981; Davies, 1932; Noback et al., 2011; Thomson and Buxton, 1923). The rationale for this geographic distribution is that alterations in nasal shape provide more efficient conditions for respiration in differing environments. In cold, dry climates, the increased surface-area-to-volume ratio and longer nasal cavity length of leptorrhine noses provides greater conditioning of inspired air by generating higher flow turbulence within the nasal passages (Noback et al., 2011). On the other hand, platyrrhine noses are more able to capture heat and moisture during expiration, necessary for enhanced heat dissipation (Franciscus and Long, 1991).

Although the postulated link between nasal index and nasal physiology is supported by anthropological studies documenting correlations between climate and nasal index, direct evidence between nasal index and measures of nasal patency have not been extensively investigated. Until recently, studies investigating the relationship between nasal index and physiologic functions such as nasal resistance have relied on rhinomanometry, acoustic rhinometry, or measurements of computed tomography (CT) or magnetic resonance imaging (MRI) scans (Babatola, 1990; Calhoun et al.,

* Corresponding author at: Division of Head and Neck Surgery & Communication Sciences, Duke University Medical Center, Box 3805, Durham, NC 27710, USA.
E-mail address: dennis.frank@duke.edu (D.O. Frank-Ito).

http://dx.doi.org/10.1016/j.resp.2016.07.004
1569-9048/

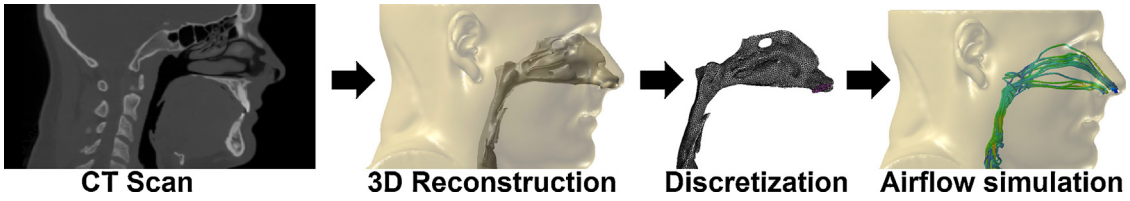

Fig. 1. Computational fluid dynamics modeling process, from CT scan to airflow simulation.

1990; Doddi and Eccles, 2011; Ohki et al., 1991; Stocks and Godfrey, 1978; Yokley, 2009). These techniques, while useful, are only able to measure a limited number of physiologic variables In the present study, computational fluid dynamics (CFD) modeling approach was used in assessing the relationship between NI and physiologic variables, such as nasal resistance, wall shear stress (a measure of air interaction with nasal mucosa) and heat flux (a measure of mucosa cooling ability).

CFD techniques provide highly detailed analyses of the effects of nasal anatomic structure on nasal function. For example, CFD has been used to model and analyze airflow and particle transport in the sinonasal cavity (Cannon et al., 2013; Choi et al., 2016; Elad et al., 2006; Frank-Ito et al., 2014a, 2015, 2016; Frank et al., 2012a,b, 2013a,b; Inthavong et al., 2006; Jo et al., 2015; Kim et al., 2014; Kimbell et al., 2013, 2012; Moghadas et al., 2011; Naftali et al., 1998; Rhee et al., 2012; Schroeter et al., 2011; Schroeter et al., 2008; Shang et al., 2015; Wen et al., 2008), as well as characterizing laryngeal flow circulation (Frank-Ito et al., 2014b; Gokcan et al., 2010; Luo et al., 2009; Mihaescu et al., 2010; Wootton et al., 2014; Xu et al., 2006). In brief, implementation of CFD methods involve (1) three dimensional (3D) reconstruction of (sino)nasal geometry from CT/MRI images; (2) generation of mesh elements in the computational domain to discretize the reconstructed geometry; (3) simulation of airflow by numerically solving the discretized equations governing fluid flow (Fig. 1).

2. Methods

2.1. Subjects and nasal model reconstruction

This is a retrospective study approved by the Duke University Health System Institutional Review Board for Clinical Investigations. Sixteen adult subjects with anatomically normal sinonasal CT scans were selected based on a search of Duke University Medical records. Inclusion criteria were normal sinonasal anatomy with septal deviation of $\leq 5^{\circ}$ in any direction including septal spurs; high resolution spiral CT scan images with ≥ 100 axial images of the sinuses; and no clinical evidence of sinonasal disease. CT images were examined by a Duke University attending radiologist and an otolaryngologist to ensure that the sinonasal cavities of all subjects selected for this work had radiographic evidence of normal nasal and paranasal cavity. 3D reconstruction of each subject's anatomy was performed using imaging analysis and segmentation software, Avizo™ 8.1 standard (FEI Visualization Sciences Group, Burlington, MA).

2.2. Mesh generation and numerical simulation

Reconstructed 3D sinonasal modes were exported from Avizo in stereolithography file format and imported into the CAD and mesh generating software package ICEM-CFD™ 14.5 (ANSYS, Canonsburg, PA). Planar inlet surfaces around the nostrils and an outlet surface at the nasopharynx were constructed to specify flow inlet and outlet. In related CFD studies, Doorly et al. (2008), Taylor et al. (2010), and Corley et al. (2012) performed simulations with inlet surface where the external nose is covered with a hemisphere under velocity inlet or plug flow boundary conditions (Zubair et al., 2012). Doorly et al. (2008) reported that inlet configuration incorporating the external face with a hemisphere covering the nose does not truncate inflow fluid predictions compared to models with planar inlet surfaces. However, in simulation setup under pressure driven boundary conditions (Zubair et al., 2012), as in the present study, because we are primarily interested in transnasal resistance, average wall shear stress and average heat flux values, we expect that the difference in these values between models with either inlet configuration will be negligible since the flow field would recover over the length of the computational domain in the nasal passage.

Following configurations of inlet and outlet surfaces in the present work, a hybrid mesh consisting of about 6 million unstructured tetrahedral elements and fine three-layer prism elements was generated in each model's computational domain. The choice of hybrid tetrahedral-prismatic mesh density chosen was consistent with a detailed mesh sensitivity study done by Frank-Ito et al. (2016) which showed that mesh independent numerical results characterized by asymptotic behavior was seen starting at 4 million elements. For this reason mesh refinement analysis was deemed unnecessary in this study. Mesh quality analysis was done to ensure that the aspect ratio for the hybrid mesh was adequately smoothed to prevent distorted elements from affecting the accuracy of the numerical simulation.

ANSYS Fluent™ 14.5 (ANSYS, Canonsburg, PA) was used to carry out CFD airflow simulations in the sinonasal passage under physiologic pressure-driven conditions to mimic actual inspiration. Although nasal airflow can sometimes become turbulent at higher flow rate occurring during sniffing or exercise, there is evidence that during resting to moderate inspiration the flow conditions are predominately laminar with Mach number$\ll 0.2$ (Sidlof and Zorner, 2013). To this end, steady-state, laminar and incompressible inspiratory airflow was simulated in each computational domain of the sinonasal airspace. Fluent™ uses the finite volume method to solve the discretized governing equations of fluid flow, given by

$$\nabla \cdot \vec{u} = 0, \tag{1.1}$$

$$\rho\left(\vec{u}\cdot\nabla\right)\vec{u} = -\nabla p + \mu\nabla^2\vec{u}, \tag{1.2}$$

$$\rho C_p\left(\vec{u}\cdot\nabla\right)T = k\nabla^2 T, \tag{1.3}$$

where $\vec{u}$ is the velocity vector, ρ is the fluid density, μ is dynamic viscosity, p is pressure, $C_p$is specific heat at constant pressure, k is thermal conductivity, and T is temperature. In this study $\rho = 1.204\text{kg/m}^3$, $\mu = 1.825\times10^{-5}$kg/m-s, $C_p = 1005$j/kg-k, and $k = 0.0268$ w/m-k. The no-slip, stationary wall boundary condition was imposed on the 3D sinonasal geometry and temperature set to 305.75 K. A "pressure-inlet" condition at the nostrils (inlet surface) with gauge pressure set to zero and temperature set to 293.15 K. And a "pressure-outlet" condition at the outlet (nasopharynx) with gauge pressure set to negative 15 Pa (constant inhalation pressure) and temperature set to 305.75 K. The rational for choosing what values to set temperature at the boundaries was based on a prior study by Lindemann et al. (2002) (see also Garcia et al. (2007)), where nasal mucosal temperature was measured during respira-